Theoretical study of Strong gravitational lensing around Dyonic ModMax black hole: constraints from EHT observations

Lola Meliyeva[1,2†] Obid Xoldorov[3‡] Olmos Tursunboyev[4§] Shavkat Karshiboev[5ǂ] Sardor Murodov[6♯]
Isomiddin Nishonov[7,8¶] Bekzod Rahmatov[9♭]

[1]Denou Institute of Entrepreneurship and Pedagogy, Surkhandarya 190500, Uzbekistan
[2]Specialized boarding school, Marvarid Street, Denau 190500, Uzbekistan
[3]Samarkand State University, University Avenue 15, Samarkand 140104, Uzbekistan
[4]Department of Physics, Jizzakh state pedagogical university Jizzakh 130100, Uzbekistan
[5]Uzbek-Finnish Pedagogical Institute, Spitamen Shokh Street 166, Samarkand 140100, Uzbekistan
[6]New Uzbekistan University, Movarounnahr Street 1, Tashkent 100007, Uzbekistan
[7]Physics and Chemistry Department, National Research University TIIAME, Kori Niyoziy 39, 100000 Tashkent, Uzbekistan
[8]Shahrisabz State Pedagogical Institute, Shahrisabz Str. 10, Shahrisabz 181301, Uzbekistan
[9]Tashkent International University of Education, Imom Bukhoriy 6, Tashkent 100207, Uzbekistan

Abstract: In this study, we investigate the properties of the Dyonic ModMax black hole solution by using strong gravitational lensing. We also calculate the time delay between two relativistic images of a background object. At the beginning, we analyze expressions for the photon orbits in the Dyonic ModMax black hole's spacetime. To obtain observational consequences, we provide expressions for the observable quantities, such as angular radius and magnifications. According to many observations, it is suggested that many nearby galaxies contain supermassive central black holes. In our model, such a supermassive black hole can be characterized by two additional parameters: γ and Q. Notably, the bending angle $\alpha_D(b)$ and the angular position θ_∞ decrease with increasing charge of the black hole Q, while the parameter γ displays behavior contrary to that of Q. By using observational data of supermassive black holes $SgrA^*$ and $M87^*$, we obtain constraints for these parameters.

Keywords: Strong gravitational lensing, Dyonic ModMax Black Hole, Milky Way, EHT

DOI: **CSTR:**

I. INTRODUCTION

The study of strong gravitational lensing provides a profound window into the nature of spacetime and the properties of black holes. This phenomenon, predicted by Einstein's theory of general relativity[1, 2], occurs when light from a distant source is bent by the gravitational field of a massive object, such as a black hole, resulting in multiple images or highly magnified and distorted images of the source[3]. Strong gravitational lensing not only offers insights into the structure and dynamics of black holes but also serves as a powerful tool for probing fundamental physics under extreme conditions[4].

In recent years, the Event Horizon Telescope (EHT) has revolutionized our understanding of black holes by capturing the images of the shadow of a supermassive black holes at the center of the galaxy $M87^*$[5, 6] and at the center of Milky Way [7, 8]. These unprecedented observations provide a unique opportunity to test various black hole models and theories of gravity[9]. Previous research has investigated the lensing properties of black holes in various modified gravity frameworks[10−14]. However, the gravitational lensing effects of black holes described by non-linear electrodynamics, such as the Dyonic ModMax model, remain underexplored.

Recent studies have explored gravitational lensing in non-linear electrodynamics, including the Dyonic ModMax model, focusing on weak lensing, plasma effects, and black hole shadows [15−20]. However, strong lensing and the interplay of dual charges with rotation remain underexplored [21, 22]. The Dyonic ModMax model's duality and conformal invariance offer unique lens-

Received 21 July 2025; Accepted 22 July 2025

† E-mail: Electronic address: lolamelieva9634@gmail.com, ixm207@piima.uz
‡ E-mail: Electronic address: obidxoldorov@gmail.com
§ E-mail: Electronic address: tursunboyevolmosbek5597@gmail.com
ǂ E-mail: Electronic address: shavkat.qarshiboyev.89@bk.ru
♯ E-mail: Electronic address: mursardor@ifar.uz
¶ E-mail: Electronic address: isomiddinniwonov96@gmail.com
♭ E-mail: Electronic address: rahmatovbekzod@samdu.uz

ing signatures [23, 24]. This study investigates strong lensing in Dyonic ModMax black holes, proposing novel observational tests to constrain model parameters using future telescope data [16, 17], addressing primary and relativistic images in the strong gravitational field regime.

The Dyonic ModMax black hole model extends the conventional Maxwell theory by incorporating a modification through nonlinear electrodynamics, leading to distinct spacetime features that are absent in other modified gravity models[25]. Among the intriguing models that have emerged is the Dyonic ModMax black hole, which incorporates modifications to Maxwell's electrodynamics, leading to novel predictions about the behavior of light and matter in the vicinity of the black hole[26−29].

This article presents a theoretical investigation of strong gravitational lensing around Dyonic ModMax black holes. By analyzing the lensing effects and comparing them with the EHT observations, we aim to place constraints on the parameters of the Dyonic ModMax black hole model. We begin by reviewing the key aspects of gravitational lensing theory[30] and the Dyonic ModMax black hole solution[29, 31−34]. Subsequently, we derive the lensing observables, such as the angular position and magnification of the lensed images, and examine how these are influenced by the unique features of the Dyonic ModMax black hole.

Our study is motivated by the need to explore alternative gravity theories and to understand how deviations from classical general relativity manifest in observational phenomena[35−43]. The Dyonic ModMax black hole serves as a test case for these explorations, providing insights that could extend to other modified gravity theories. By comparing our theoretical predictions with the empirical data from the EHT[44−53], we aim to identify distinctive signatures of the Dyonic ModMax black hole and determine the feasibility of this model in explaining the observed characteristics of black hole shadows and lensing patterns.

The results of this investigation will not only shed light on the viability of the Dyonic ModMax black hole model but also contribute to the broader effort to test the limits of general relativity and explore new physics in the strong gravity regime[40, 54−57]. Through this theoretical and observational synergy, we seek to deepen our understanding of black holes and the fundamental laws governing our universe[58−60].

In this paper, we estimate the deflection angle of the light rays and the time delay of the signals from two relativitic images. We show that time delays between relativistic images are indeed measurable in most supermassive black holes cases. Moreover, it turns out that in a first approximation, the time delay between consecutive relativistic images is proportional to the minimum impact angle. The ratio between these two observables is nothing but the distance of the lens, which can be estimated in a very precise way and without bias. This paper is structured as follows: in Sect. II we will give brief explanation about Dyonic ModMax black hole solution and obtain horizon properties, III, we will provide the main results of the gravitational lensing in the case of strong field regime. In Sect. IV we will derive a general expression for the time delay, also we will consider Dyonic ModMax spacetime case and calculate time delay for supermassive black holes at the center of several galaxies such as Milky Way, M87, NGC4649, NGC4697, and NGC5128(cenA). Finally, in Sect. V, we will give several conclusion.

II. HORIZON PROPERTIES OF DYONIC MODMAX BLACK HOLE

Dyonic ModMax black hole space-time singularities have been extensively studied in GR with NED[17, 28, 61−63]. However, here we focus on a new black hole solution in GR with NED, involving an exotic field referred to as the Dyonic ModMax field. The action can be written as

$$S = \int \sqrt{-g}\left[\frac{1}{8\pi\kappa}R + L(x,y)\right]d^4x \tag{1}$$

where

$$L(x,y) = x\cosh\gamma + \sqrt{x^2+y^2}\sinh\gamma \qquad \text{where} \tag{2}$$

$$x = \frac{1}{4}F_{\mu\nu}F^{\mu\nu} \qquad \text{and} \qquad y = \frac{1}{4}F_{\mu\nu}\tilde{F}^{\mu\nu}. \tag{3}$$

are the electromagnetic Lorentz invariants in terms of the electromagnetic tensor $F_{\mu\nu}$ and its dual $\tilde{F}_{\mu\nu} := \frac{1}{2}\epsilon_{\mu\nu\sigma\rho}F^{\sigma\rho}$. From the ModMax Lagrangian the Plebański dual variable reads [31, 64]

$$P_{\mu\nu} := -L_x F_{\mu\nu} - L_y\tilde{F}_{\mu\nu} = \left[\cosh\gamma - \frac{x}{(x^2+y^2)^{1/2}}\sinh\gamma\right]F_{\mu\nu} - \frac{y\sinh\gamma}{(x^2+y^2)^{1/2}}\tilde{F}_{\mu\nu}.$$

Its dual is

$$\tilde{P}_{\mu\nu} = \left[\cosh\gamma - \frac{x}{(x^2+y^2)^{1/2}}\sinh\gamma\right]\tilde{F}_{\mu\nu} + \frac{y\sinh\gamma}{(x^2+y^2)^{1/2}}F_{\mu\nu}.$$

Modified Maxwell field equations is given by[29]:

$$\nabla_\mu P^{\mu\nu} = 0. \tag{4}$$

Also the Einstein equations can be expressed as

$$R^{\mu}_{\nu} - \frac{1}{2}\delta^{\mu}_{\nu}R + \Lambda\delta^{\mu}_{\nu} = 8\pi T^{\mu}_{\nu} \tag{5}$$

Here, the energy momentum tensor T^{μ}_{ν} is given by [29, 31]

$$8\pi T^{\mu}_{\nu} = -F^{\mu\beta}P_{\beta\nu} + \delta^{\mu}_{\nu}L = F^{\mu\beta}(L_x F_{\beta\nu} + L_y \tilde{F}_{\beta\nu}) + \delta^{\mu}_{\nu}L \tag{6}$$

To solve the einstein equation, we choose following anzats

$$ds^2 = -f(r)dt^2 + f(r)^{-1}dr^2 + r^2(d\theta^2 + \sin^2\theta d\phi^2), \tag{7}$$

In this paper we consider only asymptotically flat configurations, so that we choose $\Lambda = 0$ in Eq.(5). First we take $A_{\mu} = (\Phi(r), 0, 0, Q_m \cos\theta)$ to consider dyonic solution. In this case we get

$$F_{\mu\nu} = -\Phi_{I,r}\delta^{0}_{[\mu}\delta^{1}_{\nu]} - Q_m \sin\theta \delta^{2}_{[\mu}\delta^{3}_{\nu]}. \tag{8}$$

In consequence

$$x = \frac{1}{2}\left(-\Phi^2_{,r} + \frac{Q^2_m}{r^4}\right),\ y = -\frac{\Phi_{,r}Q_m}{r^2},$$
$$(x^2 + y^2)^{1/2} = \frac{1}{2}\left(-\Phi^2_{,r} + \frac{Q^2_m}{r^4}\right), \tag{9}$$

and it is straightforward to show that, the only non-vanishing Pleban'ski variables are

$$P_{01} = -(\cosh\gamma + \sinh\gamma)\Phi_{,r} = -e^{\gamma}\Phi, r$$
$$P_{23} = -(\cosh\gamma - \sinh\gamma)Q_m \sin\theta = -e^{-\gamma}Q_m \sin\theta \tag{10}$$

For the electric potential, we can write

$$\Phi(r) = \frac{Q_e \cdot e^{-\gamma}}{r}. \tag{11}$$

This condition leads to set conservation low for P_{01}. In this case, the gravitational field equations read

$$-\frac{m_{,r}}{r^2} = -\frac{(Q^2_e + Q^2_m)\cdot e^{-\gamma}}{2r^4}$$
$$-\frac{m_{,rr}}{2r} = \frac{(Q^2_e + Q^2_m)\cdot e^{-\gamma}}{2r^4} \tag{12}$$

the solution of this system of equations is

$$m(r) = M - \frac{(Q^2_e + Q^2_m)\cdot e^{-\gamma}}{2r}. \tag{13}$$

Finally, we can find the lapse function of the metric Eq.(7)

$$f(r) = 1 - \frac{2M}{r} + \frac{(Q^2_e + Q^2_m)\cdot e^{-\gamma}}{r^2}, \tag{14}$$

where Q_e and Q_m are the electric and magnetic charge of the black hole respectively, γ is related to a constant screening factor for the charge of the black hole, corresponds to the nonlinear parameter [29, 34]. If we choose $\gamma = 0$, Maxwell's theory is recovered. Also, by choosing $Q_e = Q_m = 0$ we can easily get the Schwarzschild case. To analyse horizon properties such a black hole, we set $f(r) = 0$. Under this condition we can find the event horizon radius:

$$r_h = M \pm \sqrt{\left(M^2 - (Q^2_e + Q^2_m)\right)\cdot e^{-\gamma}} \tag{15}$$

Throughout this paper we study only photon motion which is neutral, massless particle. So we can define Q as $Q^2_e + Q^2_m = Q^2$.From Eq.(15) we can obtain the maximum value of black holes charge:

$$0 < Q < M \cdot e^{-\gamma/2} \tag{16}$$

From Eq.(15) one can easily find that Q and γ parameters negatively affect on the horizon radius. Also, Eq.(16) gives boundary values for charge Q in terms of M and γ.

III. STRONG GRAVITATIONAL LENSING OF DYONIC MODMAX BLACK HOLE

In this section, we have investigated strong gravitational lensing effect in the spacetime described as Eq.(7). To find photon sphere radius we can use following expression [65]:

$$\frac{g'_{\theta\theta}(r)}{g_{\theta\theta}(r)} - \frac{g'_{tt}(r)}{g_{tt}(r)} = 0, \tag{17}$$

where $'$ is the differentiation with respect to the radial coordinate r. From Eqs.(7) and (17), we get

$$r_m = \frac{3M + \sqrt{9M^2 - 8Q^2e^{-\gamma}}}{2}. \tag{18}$$

The specific energy and angular momentum can be written as

$$E \equiv -g_{\mu\nu}t^{\mu}\kappa^{\nu} = \frac{\Delta}{r^2}\dot{t}, \tag{19}$$

and

$$L \equiv g_{\mu\nu}\phi^{\mu}\kappa^{\nu} = r^2\dot{\phi} \tag{20}$$

where $\Delta = f(r)\cdot r^2$ and κ_{μ} is the killing vector. One of the important quantity is impact parameter which is defined as

$$b \equiv \frac{L}{E} = \frac{r^4\dot{\phi}}{\Delta\dot{t}}. \tag{21}$$

We also assume the motion occurs in the equatorial plane, $\theta = \pi/2$. With this assumption, equations of motion in the radial direction can be obtained as

$$\dot{r}^2 = \frac{\Delta^2}{r^4}\dot{t}^2 - \Delta\dot{\phi}^2, \tag{22}$$

or

$$\dot{r}^2 = V(r), \tag{23}$$

where $V(r)$ is the effective potential for the motion of the photon and it reads

$$V(r) \equiv E^2 - \frac{\Delta}{r^4}L^2. \tag{24}$$

We consider that light beam coming from infinity is deflected at the closest distance $r = r_0$ and goes to infinity. At the closest distance, $\dot{r}$ vanishes and from Eq.(22) we get following formula for the critical impact parameter at the closest distance as [65]

$$b(r_0) = \frac{r_0^2}{\sqrt{\Delta(r_0)}}. \tag{25}$$

By using the above equation, we can define critical impact parameter as

$$b_c(r_m) \equiv \lim_{r_0\to r_m} b(r_0) = \lim_{r_0\to r_m} \frac{r_o^2}{\sqrt{\Delta(r_0)}}. \tag{26}$$

The meaning of critical impact parameter is that if the photons that have an impact parameter $b < b_c$ fall into the black hole. Parameter $b(r_0)$ can be expanded in the power of $r_0 - r_m$ as

$$b(r_0) = b_c(r_m) + \frac{3Mr_m - 4Q^2e^{-\gamma}}{2(Mr_m - \epsilon M^2)^{\frac{3}{2}}}(r_0 - r_m)^2 + O((r_0 - r_m)^3). \tag{27}$$

From Eq.(22), we can find following relationship between r and ϕ

$$\left(\frac{dr}{d\phi}\right)^2 = r^4\left(\frac{1}{b^2} - \frac{\Delta}{r^4}\right), \tag{28}$$

or we can write in terms of the deflection angle $\alpha(r_0)$ of the light beam

$$\alpha = I(r_0) - \pi, \tag{29}$$

where

$$I(r_0) \equiv 2\int_{r_0}^{\infty} \frac{dr}{r^2\sqrt{\frac{1}{b^2} - \frac{\Delta}{r^4}}}. \tag{30}$$

By introducing a variable z defined as

$$z \equiv 1 - \frac{r}{r_0}, \tag{31}$$

$I(r_0)$ can be rewritten as

$$I(r_0) = \int f(z, r_0)dz, \tag{32}$$

where

$$f(z, r_0) = \frac{2r_0}{\sqrt{c_1(r)z + c_2(r_0)z^2 + c_3(r_0)z^3 + c_4(r_0)z^4}}, \tag{33}$$

$$c_1(r_0) \equiv 2(r_0^2 - 3Mr_0 + 2Q^2e^{-\gamma}), \tag{34}$$

$$c_2(r_0) \equiv -r_0^2 + 6Mr_0 - 6Q^2e^{-\gamma}, \tag{35}$$

$$c_3(r_0) \equiv -2Mr_0 + 46Q^2e^{-\gamma}, \tag{36}$$

$$c_4(r_0) \equiv -Q^2e^{-\gamma}. \tag{37}$$

$I(r_0)$ can be splitted into two parts, i.e., a divergent part $I_D(r_0)$ and a regular part $I_R(r_0)$: I(r_0) = $I_D(r_0)$+ $I_R(r_0)$. The divergent part is expressed as

$$I_D(r_0) = \int_0^1 f_D(z, r_0)\,dz, \tag{38}$$

where

$$f_D(z, r_0) = \frac{2r_0}{\sqrt{c_1(r_0)z + c_2(r_0)z^2}}, \tag{39}$$

and the result is

$$I_D(r_0) = \frac{4r_0}{\sqrt{-r_0^2+6Mr_0-6Q^2e^{-\gamma}}} \log\frac{\sqrt{-r_0^2+6Mr_0-6Q^2e^{-\gamma}}+\sqrt{r_0^2-2Q^2e^{-\gamma}}}{2(r_0^2-3Mr_0+2Q^2e^{-\gamma})}. \quad (40)$$

In the strong deflection limit $r_0 \to r_m$ Eq.(40) is formulated as

$$I_D(b) = -\bar{a}log\left(\frac{b}{b_c}-1\right)+\bar{a}log\frac{2(3Mr_m-4Q^2e^{-\gamma})}{Mr_m-Q^2e^{-\gamma}}+ O((b-b_c)log(b-b_c)), \quad (41)$$

where $\bar{a}$ is given by

$$\bar{a} = \frac{r_m}{\sqrt{3Mr_m-4Q^2e^{-\gamma}}} \quad (42)$$

Additionally, the regular part I_R is defined as

$$I_R(r_0) \equiv \int_0^1 f_R(z,r_0)\,dz, \quad (43)$$

where

$$f_R(z,r_0) \equiv f(z,r_0) - f_D(z,r_0). \quad (44)$$

Since we are investigating deflection angle in the strong field limit $r_0 \to r_m$, we consider

$$\lim_{r_0\to r_m} f_R(z,r_0) = \frac{2r_m}{z\sqrt{c_2(r_m)+c_3(r_m)z+c_4(r_m)z^2}} - \frac{2r_m}{z\sqrt{c_2(r_m)}} \quad (45)$$

After some calculations, the analytical expression can be taken as

$$I_R(b) = \bar{a}\log\left[\frac{4(3Mr_m-4Q^2e^{-\gamma})^2}{M^2r_m^2(Mr_m-Q^2e^{-\gamma})}\times(2\sqrt{Mr_m-Q^2e^{-\gamma}} - \sqrt{3Mr_m-4Q^2e^{-\gamma}})^2\right] + O((b-b_c)\log(b-b_c)). \quad (46)$$

Eventually, the bending angle of the light rays $\alpha(b)$ in the strong deflection limit $b \to b_c$ is given by [65]

$$\alpha(b) = -\bar{a}\log\left(\frac{b}{b_c}-1\right)+\bar{b}+O\left((b-b_c)log(b-b_c)\right), \quad (47)$$

where $\bar{a}$ and $\bar{b}$ as

$$\bar{a} = \frac{r_m}{\sqrt{3Mr_m-4Q^2e^{-\gamma}}} \quad (48)$$

$$\bar{b} = \bar{a}\log\left[\frac{8(3Mr_m-4Q^2e^{-\gamma})^2}{M^2r_m^2(Mr_m-Q^2e^{-\gamma})^2}\times\left(2\sqrt{Mr_m-M^2}-\sqrt{3Mr_m-4Q^2e^{-\gamma}}\right)^2\right]-\pi \quad (49)$$

respectively. Table 1 gives information about b_c/M, $\bar{a}$ and $\bar{b}$ are the lensing coefficients as the functions of the charge of the black hole Q/M and γ parameters. When the black hole non-charged $(Q/M=0)$, we obtain $b_c = 3\sqrt{3}M$, $\bar{a}=1$, and $\bar{b}=-0.40023$. When the black hole has $Q/M=0.6$, we obtain $b_c = 4.59M$, $\bar{a}=1.1092$ and $\bar{b}=-0.4085$ which means in the case of Dyonic ModMax black hole, the quantity b_c will be smaller than the Schwarzschild case. From Fig. 1, One can see that the coefficient $\bar{a}$ increases while $\bar{b}$, b_c, r_m decrease with the increased value of Q/M. The deflection angle $\alpha_D(b)$ as a function of b for different Q/M and γ is depicted in Fig. 2 The deflection angle for Dyonic ModMax black holes (see Fig. 2) is monotonically decreasing with impact parameter b and deflection angle $\alpha_D(b) \to \infty$ as $b \to b_c$. Interestingly, the deflection angle for Dyonic ModMax black holes decreases with the increasing value of parameter b whereas for an impact parameter close to the critical impact parameter (see Fig. 2), the deflection angle $\alpha_D(b)$ decreases in both cases increasing values of Q/M and γ parameters.

$$\beta = \theta - \frac{D_{LS}}{D_{OS}}\Delta\alpha_n \quad (50)$$

Where $\Delta\alpha = \alpha - 2n\pi$ is the offset of deflection angle looping over $2n\pi$ and n is an integer. Here, β is the angular position of the source while θ is the angular position of the image from the optic axis. The distance between the observer and the lens and between the observer and the source are D_{OL} and D_{OS}, respectively. Using Eqs. (47) and (50), the position of the nth relativistic image can be

Table 1. Estimated for the strong lensing coefficients $\bar{a}$, $\bar{b}$ and the critical impact parameter b_c/R for Dyonic ModMax Black hole Spacetime. The values for $Q/M=0$ and $\gamma=0$ correspond to a Schwarzschild black hole.

γ	Q/M	$\bar{a}$	$\bar{b}$	b_c/R_s
0	0.0	1	-0.40023	2.59808
-0.5	0.4	1.03512	-0.396203	2.47728
-0.5	0.8	1.58337	-1.08685	1.94022
0.0	0.4	1.01974	-0.397184	2.49912
0.0	0.8	1.12317	-0.413638	2.27299
0.5	0.4	1.01147	-0.398215	2.55523
0.5	0.8	1.05727	-0.396916	2.41483

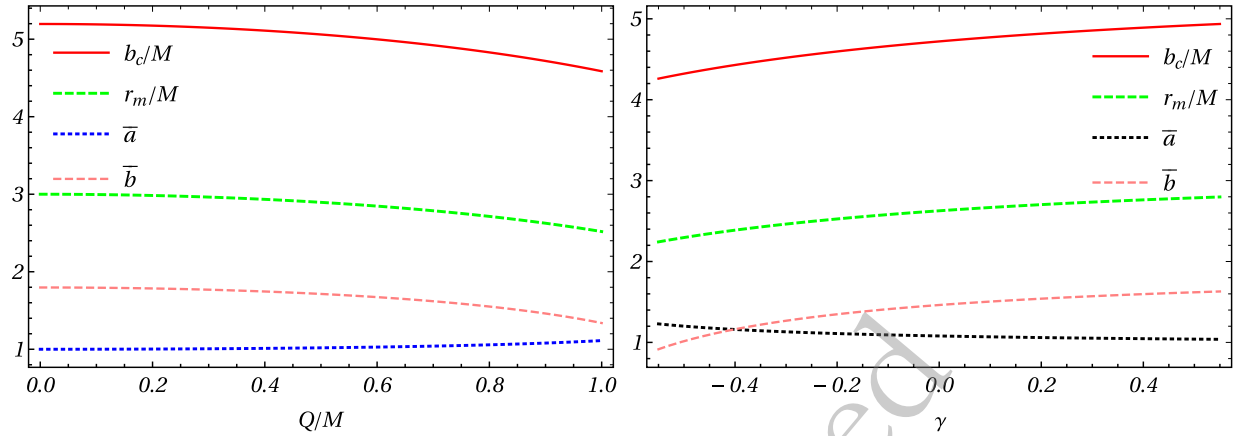

Fig. 1. The quantities $b_c/M, r_m/M, \bar{a}$, and $\bar{b}$ in the Dyonic ModMax spacetime as the functions of Q/M and γ. $\bar{a}=1$ and $\bar{b}=-0.4002$ at $Q/M=0, \gamma=0$ correspond to the values of a Schwarzschild black hole.

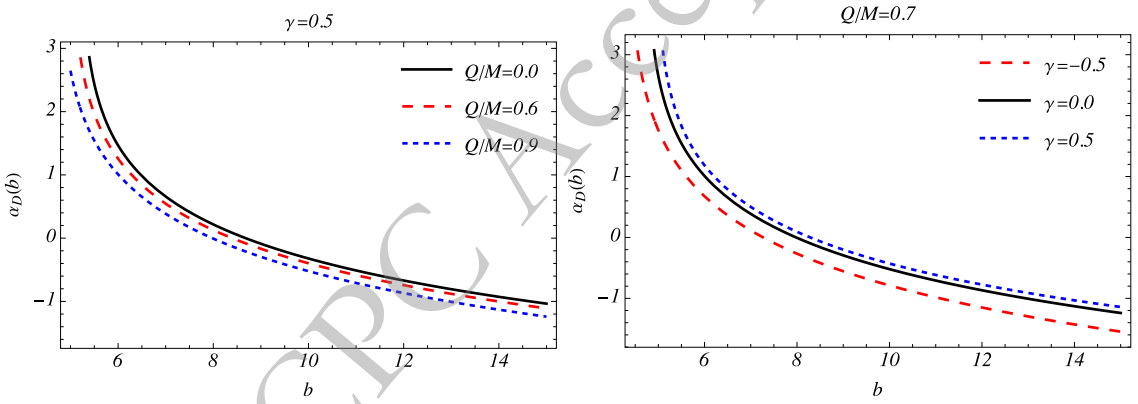

Fig. 2. Variation of deflection angle for Dyonic ModMax black hole spacetime as a function of the impact parameter b for different values of parameters Q/M(left) and γ (right)

approximated as [65]

$$\theta_n = \theta_n^0 + \frac{b_c e_n(\beta-\theta_n^0)D_{OS}}{\bar{a}D_{LS}D_{OL}}, \tag{51}$$

Where

$$e_n = e^{\left(\frac{\bar{b}}{\bar{a}}-\frac{2n\pi}{\bar{a}}\right)}, \tag{52}$$

θ_n^0 are are the image positions corresponding to $\alpha = 2n\pi$.As gravitational lensing conserves surface brightness, the magnification is the quotient of the solid angles subtended by the nth image and the source ([66],[65], [67]). The magnification of the nth relativistic image reads as [65]

$$\mu_n = \left(\frac{\beta}{\theta}\frac{d\beta}{d\theta}\right)^{-1} = \frac{b_c^2 e_n(1+e_n)D_{OS}}{\bar{a}\beta D_{LS}D_{OL}^2} \tag{53}$$

The first relativistic image is the brightest one, and the magnifications decrease exponentially with n. The magnifications are proportional to $1/D_{OL}^2$ which is a very small factor and thus the relativistic images are very faint, unless β has values close to zero, i.e., nearly perfect alignment. Having obtained the deflection angle (Eq.(47), (48), and (49)), we calculate three observables of relativistic images (see Table 3, Fig. 3,4 and 5), the angular position of the asymptotic relativistic images (θ_∞), the angular separation between the outermost and asymptotic relativistic images(s_∞), (see Fig. 4) and relative magnification of the outermost relativistic image with other relativistic images (r_{mag})(see Fig. 5)[65].

$$\theta_\infty = \frac{b_c}{D_{OL}} \tag{54}$$

$$s = \theta_1 - \theta_\infty = \theta_\infty e^{\left(\frac{\bar{b}}{\bar{a}}-\frac{2n\pi}{\bar{a}}\right)}, \tag{55}$$

$$r_{mag} = \frac{5\pi}{\bar{a}\log 10}. \tag{56}$$

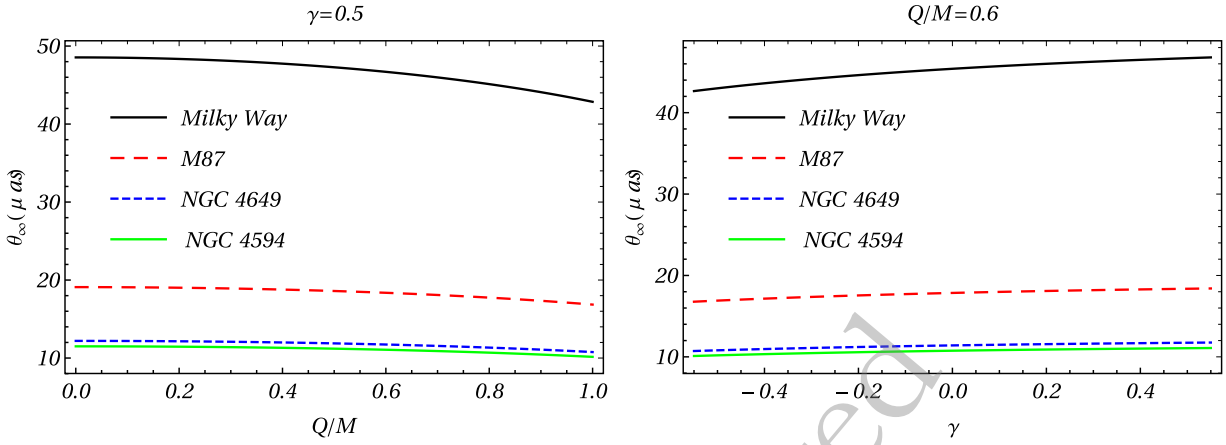

Fig. 3. Behavior of lensing observables θ_∞ as a function of parameters Q/M and γ in strong field limit by considering that the space-time around the compact object.

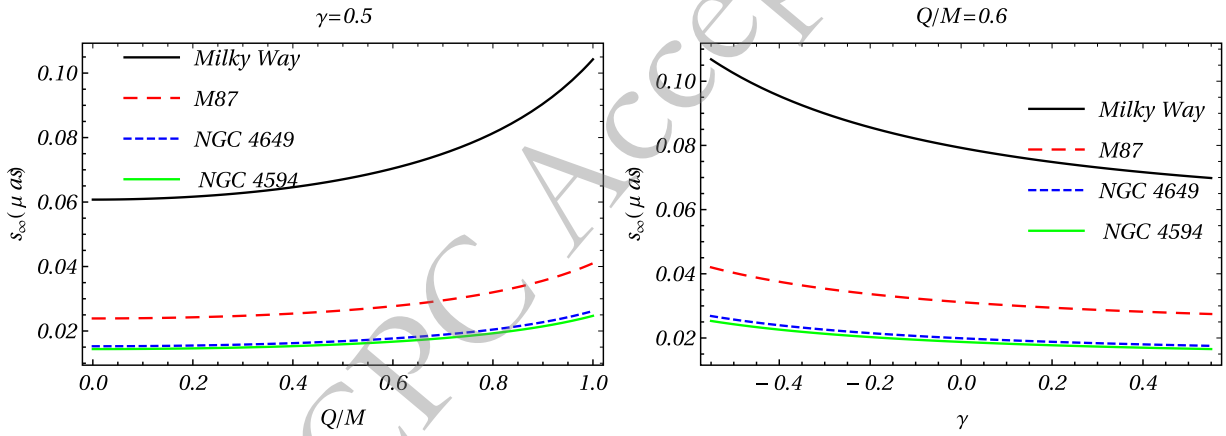

Fig. 4. Behavior of lensing observables s_∞ as a function of parameters Q/M and γ in strong field limit by considering that the space-time around the compact object.

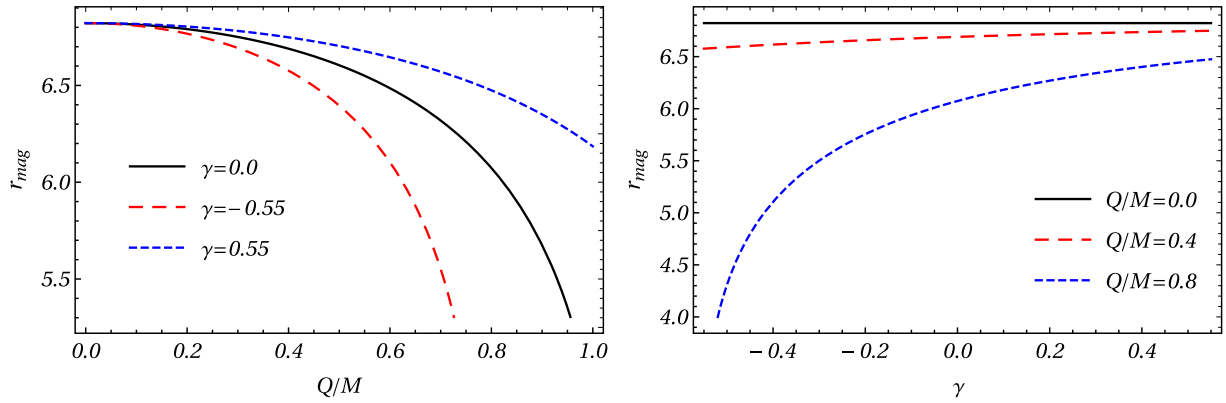

Fig. 5. This graph shows the relationship between the contact parameter r_{mag} and the parameter ϵ.

The strong deflection limit coefficients $\bar{a}$, $\bar{b}$ and the critical impact parameter ups can be obtained after measuring s, r_{mag}, and θ_∞. If θ_∞ represents the asymptotic position of a set of images in the limit $n \to \infty$, we consider that only the outermost image θ_1 is resolved as a single image and all the remaining ones are packed together at θ_∞. The values obtained from measurements can be compared with those predicted by the theoretical models to check the nature of the black hole. Table 3 presents the observable values corresponding to various parameters γ

Table 2. The angular position of the asymptotic relativistic images (θ_∞), the angular separation between the outermost and asymptotic relativistic images (s_∞), and relative magnification of the outermost relativistic image with other relativistic images (r_{mag}) for Milky Way, NGC4486, and NGC4649 in the case of fixed the charge of the black hole Q/M and γ parameters.

γ	Q/M	Milky Way		NGC4486		NGC4649		r_{mag}
		$\theta_\infty(\mu as)$	$S(\mu as)$	$\theta_\infty(\mu as)$	$S(\mu as)$	$\theta_\infty(\mu as)$	$S(\mu as)$	
0.0	0.0	48.5447	0.0607535	19.0935	0.0238954	12.1986	0.0152665	6.82188
-0.5	0.4	46.2876	0.0729555	18.2057	0.0286946	11.9974	0.0183327	6.59044
-0.5	0.8	36.2528	0.345028	14.2589	0.135705	11.3382	0.0867007	4.30845
0.0	0.4	47.2071	0.067439	18.5674	0.0265249	11.8625	0.0169465	6.68985
0.0	0.8	42.4706	0.109304	16.7044	0.0429911	10.6723	0.0274666	6.07378
0.5	0.4	47.744	0.0645842	18.7786	0.0254021	11.9974	0.0162291	6.74453
0.5	0.8	45.1208	0.081358	17.7468	0.0319995	11.3382	0.0204441	6.45234

Table 3. The time delay between two relativistic images of different galaxies.

Galaxy	M($M_\odot$)	D_{OL}(Mpc)	M/D_{OL}	$\Delta T^S_{2,1}(Schw)$	$\Delta T^S_{2,1}(DM)$
Milky Way	3.61×10^6	0.00762	2.26467×10^{-11}	11.4968	8.748
"NGC4486(M87)"	3.0×10^9	16.1	8.90733×10^{-12}	8021	7270
NGC4649	2.0×10^9	16.8	5.6908×10^{-12}	8021	7270
NGC4697	1.7×10^8	11.7	6.94569×10^{-13}	5347.34	4846.67
NGC5128(cenA)	2.4×10^8	4.2	2.73158×10^{-12}	454.53	411.97

and Q. It is evident from these results that the Dyonic ModMax black hole exhibits unique and distinguishable observable characteristics compared to other configurations.

One of the important conclusions in study of deflection angle is that we can constrain Dyonic ModMax spacetime parameter by using EHT observation. From Eq.(54), we can ascertain the specific values of these parameters that may be used to align the diameters of the M87* and Sgr A* BH, as determined by the EHT. The angular size of the image of BH M87* is reported to be $\theta_d = 42 \pm 3\mu as$. The mass and distance of M87* from the solar system are given as $M = 6.5\times10^9 M_\odot$ and $d = 16.8$ Mpc, respectively, as mentioned in Refs[7, 68]. The constraints on M87* are depicted in the left panel of Fig. 6. This figure reveals that the allowed region for the charge is quite limited when the γ parameter is negative, whereas it becomes significantly broader for positive values of γ. More specificly, the parameter constraints are: $0.7 \geq Q > 0.4$ and $\gamma \geq -0.5$. The observational data of the supermassive BH Sgr A* may be analyzed using the same methodology. A study conducted by Akiyama et al. (2019) determined that the angular diameter of the shadow of the BH Sgr A* is around $\theta_d = 48.7 \pm 7\mu as$, and its mass is estimated to be around $M \simeq 4\times10^6 M_\odot$. The distance from Earth is approximately estimated to be $d \simeq 8kpc$. The results for Sgr A* are demonstrated in Fig. 6, right panel. Analyzing this graph, it is evident that the allowed parameter region for Sgr A* is broader compared to that of the M87* observational results which are : $Q \geqslant 0.3$ and $\gamma \geqslant -0.5$. This broader range can likely be attributed to the greater observational uncertainties associated with Sgr A*.

IV. TIME DELAY IN STRONG FIELD LIMIT

The time difference is caused by the photon taking different paths while winding the black hole, so there is a time delay between different images. If we can distinguish the time signals of the first image and other packed images. The time spent by the photon to wind around the black hole is [69]

$$\tilde{T}(b) = \bar{a}\log\left(\frac{b}{b_c} - 1\right) + \bar{b} + O(b - b_c) \tag{57}$$

The images are highly demagnified, and the separation between the images is of the order of microarcseconds, so we must at least distinguish the outermost relativistic image from the rest, and we assume the source to be variable, which generally is abundant in all galaxies, otherwise, there is no time delay to measure. For spherically symmetric black holes, the time delay between the first and second relativistic image [69]

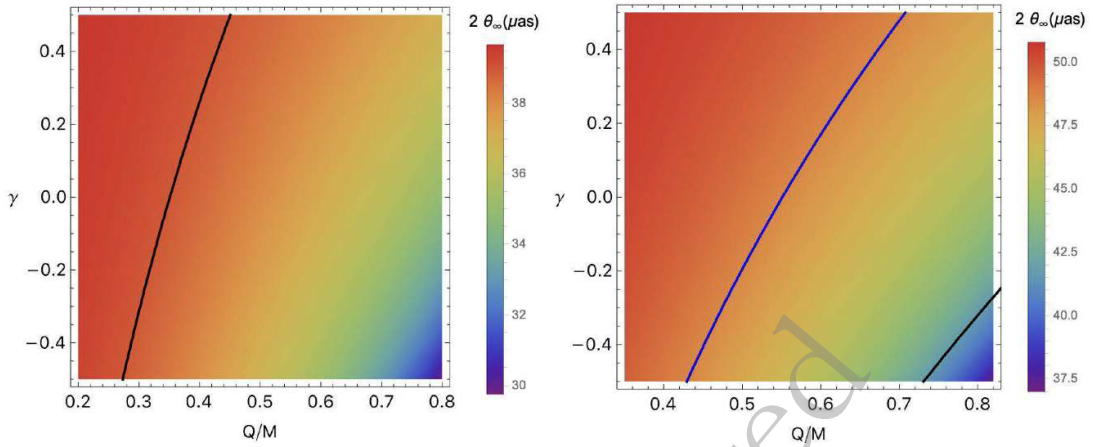

Fig. 6. Constraining parameter by using EHT observation for $M87^*$ (left panel) and $SgrA^*$ (right panel). The black thick line corresponds to the maximum values of parameters which consistent with observational results $39\mu as$ for $M87^*$(left panel) and $41.7\mu as$ for $SgrA^*$(right panel) while the blue one represents the middle value of observational results($48.7\mu as$ for $SgrA^*$).

$$\Delta T^s_{2,1} = 2\pi b_c = 2\pi D_{OL}\theta_\infty \tag{58}$$

Using Eq.(58), if we can measure the time delay with an accuracy of and the critical impact parameter with negligible error, we can obtain the distance of the black hole with an accuracy of. In Table 3, we compare several galaxies representing Schwarzschild and Dyonic ModMax spacetime. In the Dyonic ModMax spacetime spacetime, the time delays $\Delta T^s_{2.1}$ between two distinct relativistic images are comparatively smaller than the fixed value of Q/M and γ in the Schwarzschild cases. We have also analytically derived the time delays $\Delta T^s_{2.1}$ between the first and second-order relativistic images for various astronomical objects including the Milky Way, M87, NGC4649, NGC4697, and NGC5128(cenA) with the help of data are obtained from [67]. From this analysis, we have shown that if we have an independent observation for the time delay, we can strongly constrain the Dyonic ModMax space time parameters Q and γ due to measurable difference on the value of time delay.

V. CONCLUSION

Through this investigations, we can show several important notices as a conclusion:

- The radius of the spherical photon orbit r_m, the critical impact parameter b_c, the lensing coefficient $\bar{b}$, the deflection angle $\alpha_D(b)$, and the angular position θ_∞ all decrease as Q increases, while the lensing coefficient $\bar{a}$ and angular separation s_∞ exhibit the opposite trend. Consequently, the parameter γ behaves inversely to Q.
- Additionally, we have shown the constraining Dyonic ModMax spacetime with EHT observations. We represent it as parametric space graphs.
- We have also analytically derived the time delays $\Delta T^s_{2.1}$ between first and second-order relativistic images for the Milky Way, M87, NGC4649, NGC4697, and NGC5128(cenA). One can observe that for supermassive black hole with higher mass, the time delay is higher than for the case of lighter black holes.
- Based on the graphical and tabular results, the dependence of the deflection angle on the parameters Q and γ was revealed. In particular, it was observed that when γ takes negative values, the deflection angle decreases more sharply, while positive values of γ tend to smooth out this variation. Observations from the EHT, especially those related to the shadow diameters of the $M87^*$ and $SgrA^*$ black holes, were used to establish experimental constraints on these parameters. For $M87^*$, the parameters are constrained by $0.7 \geq Q > 0.4$ and $\gamma \geq -0.5$, whereas for $SgrA^*$, the allowed parameter space is broader, i.e $Q \geqslant 0.3$ and $\gamma \geqslant -0.5$, due to larger observational uncertainties.

References

[1] C. M. Will, Living Reviews in Relativity **9**, 3 (2006)
[2] C. M. Will, Living Reviews in Relativity **17**, 4 (2014)
[3] P. Schneider, J. Ehlers, and E. E. Falco, Gravitational Lenses. 1992.
[4] M. Bartelmann, Classical and Quantum Gravity **27**, 233001 (2010)
[5] K. Akiyama and *et al.* (Event Horizon Telescope Collaboration), Astrophys. J. **910**, L12 (2021)
[6] K. Akiyama and *et al.* (Event Horizon Telescope Collaboration), Astrophys. J. **910**, L13 (2021)
[7] K. Akiyama and *et al.* (Event Horizon Telescope Collaboration), Astrophys. J. **875**, L1 (2019)
[8] K. Akiyama and *et al.* (Event Horizon Telescope Collaboration), Astrophys. J. **875**, L3 (2019)
[9] C. Goddi, H. Falcke, M. Kramer, L. Rezzolla, C. Brinkerink, T. Bronzwaer, J. R. J. Davelaar, R. Deane, M.

De Laurentis, G. Desvignes, and *et al.*, International Journal of Modern Physics D **26**, 1730001 (2017)
[10] X. Jiang, X. Ren, Z. Li, Y.-F. Cai, and X. Er, "Exploring f(T) gravity via strongly lensed fast radio bursts, ", vol. 528, pp. 1965–1978, Feb. 2024.
[11] X.-M. Kuang, Z.-Y. Tang, B. Wang, and A. Wang, Phys. Rev. D **106**, 064012 (2022)
[12] S.-S. Zhao and Y. Xie, European Physical Journal C **77**, 272 (2017)
[13] S. Chen and J. Jing, Classical and Quantum Gravity **27**, 225006 (2010)
[14] T. L. Smith, "Testing gravity on kiloparsec scales with strong gravitational lenses, " *arXiv e-prints*, p. arXiv: 0907.4829, July 2009.
[15] A. Ditta, X. Tiecheng, F. Atamurotov, G. Mustafa, and M. M. Aripov, Chin. J. Phys. **83**, 664 (2023)
[16] R. C. Pantig, L. Mastrototaro, G. Lambiase, and A. Övgün, Eur. Phys. J. C **82**(12), 1155 (2022)
[17] S. I. Kruglov, Int. J. Mod. Phys. D **31**(04), 2250025 (2022)
[18] Z. Turakhonov, F. Atamurotov, A. Ovgun, A. Abdujabbarov, and S. Urinov, Commun. Theor. Phys. **76**(11), 115401 (2024)
[19] B. Rahmatov, M. Zahid, S. U. Khan, J. Rayimbaev, I. Ibragimov, Z. Yuldoshev, A. Dauletov, and S. Muminov, Chin. Phys. C **49**(7), 075105 (2025)
[20] A. Al-Badawi, Y. Sekhmani, and K. Boshkayev, Phys. Dark Univ. **48**, 101865 (2025)
[21] H. P. Saikia, M. M. Gohain, and K. Bhuyan, "Dynamics of Geodesics in Non-linear Electrodynamics Corrected Black Hole and Shadows of its Rotating Analogue, " 4 2025.
[22] D. Flores-Alfonso, B. A. González-Morales, R. Linares, and M. Maceda, Phys. Lett. B **812**, 136011 (2021)
[23] K. Karshiboev, F. Atamurotov, A. Övgün, A. Abdujabbarov, and E. Karimbaev, New Astron. **109**, 102200 (2024)
[24] B. Eslam Panah, PTEP **2024**(2), 023E01 (2024)
[25] H. Kim, Phys. Rev. D **61**, 085014 (2000)
[26] M. Born and L. Infeld, Proc. Roy. Soc. Lond. A **144**(852), 425 (1934)
[27] G. W. Gibbons, AIP Conf. Proc. **589**(1), 324 (2001)
[28] I. Bandos, K. Lechner, D. Sorokin, and P. K. Townsend, Phys. Rev. D **102**, 121703 (2020)
[29] D. Flores-Alfonso, B. A. González-Morales, R. Linares, and M. Maceda, Physics Letters B **812**, 136011 (2021)
[30] V. Perlick, Living Reviews in Relativity **7**, 9 (2004)
[31] G. W. Gibbons and C. A. R. Herdeiro, Class. Quant. Grav. **18**, 1677 (2001)
[32] G. W. Gibbons and C. A. R. Herdeiro, Class. Quant. Grav. **18**, 1677 (2001)
[33] R. Ruffini, Y.-B. Wu, and S.-S. Xue, Phys. Rev. D **88**, 085004 (2013)
[34] B. P. Kosyakov, Phys. Lett. B **810**, 135840 (2020)
[35] T. Clifton, P. G. Ferreira, A. Padilla, and C. Skordis, "Modified gravity and cosmology, ", vol. 513, pp. 1–189, Mar. 2012.
[36] C. G. Böhmer and E. Jensko, Phys. Rev. D **104**, 024010 (2021)
[37] S. Nojiri and S. D. Odintsov, "Unified cosmic history in modified gravity: From F(R) theory to Lorentz non-invariant models, ", vol. 505, pp. 59–144, Aug. 2011.
[38] T. P. Sotiriou and S.-Y. Zhou, "Black hole hair in generalized scalar-tensor gravity," Phys. Rev. Let., vol. 112, Jun 2014.
[39] S. Capozziello and M. de Laurentis, "Extended Theories of Gravity, ", vol. 509, pp. 167–321, Dec. 2011.
[40] E. Berti and *et al.*, Classical and Quantum Gravity **32**, 243001 (2015)
[41] A. De Felice and S. Tsujikawa, Living Reviews in Relativity **13**, 3 (2010)
[42] K. Koyama, Reports on Progress in Physics **79**, 046902 (2016)
[43] L. Heisenberg, "A systematic approach to generalisations of General Relativity and their cosmological implications, ", vol. 796, pp. 1–113, Mar. 2019.
[44] J. Rayimbaev, R. C. Pantig, A. Övgün, A. Abdujabbarov, and D. Demir, Annals of Physics **454**, 169335 (2023)
[45] B. Puliçe, R. C. Pantig, A. Övgün, and D. Demir, Classical and Quantum Gravity **40**, 195003 (2023)
[46] S. Vagnozzi, R. Roy, Y.-D. Tsai, L. Visinelli, M. Afrin, A. Allahyari, P. Bambhaniya, D. Dey, S. G. Ghosh, P. S. Joshi, K. Jusufi, M. Khodadi, R. K. Walia, A. Övgün, and C. Bambi, Classical and Quantum Gravity **40**, 165007 (2023)
[47] A. Uniyal, R. C. Pantig, and A. Övgün, Physics of the Dark Universe **40**, 101178 (2023)
[48] R. C. Pantig and A. Övgün, Annals of Physics **448**, 169197 (2023)
[49] F. Atamurotov, U. Papnoi, and K. Jusufi, Classical and Quantum Gravity **39**, 025014 (2022)
[50] E. Ghorani, B. Puliçe, F. Atamurotov, J. Rayimbaev, A. Abdujabbarov, and D. Demir, Eur. Phys. J. C **83**, 318 (2023)
[51] H. Hoshimov, O. Yunusov, F. Atamurotov, M. Jamil, and A. Abdujabbarov, Physics of the Dark Universe **43**, 101392 (2024)
[52] R. Kumar, S. U. Islam, and S. G. Ghosh, European Physical Journal C **80**, 1128 (2020)
[53] S. U. Islam, R. Kumara, and S. G. Ghosha, J. Cosmol. A. P **2020**, 030 (2020)
[54] D. Psaltis, Living Reviews in Relativity **11**, 9 (2008)
[55] E. Berti, V. Cardoso, and A. O. Starinets, Classical and Quantum Gravity **26**, 163001 (2009)
[56] D. Psaltis and *et al.*, Phys. Rev. Lett. **125**, 141104 (2020)
[57] N. K. Johnson-McDaniel, "Summary of Tests of General Relativity with the Binary Black Hole Signals from the LIGO-Virgo Catalog GWTC-1, " in *54th Rencontres de Moriond on Gravitation*, 5 2019.
[58] S. W. Hawking and G. F. R. Ellis, The large-scale structure of space-time. 1973.
[59] K. S. Thorne, Black holes and time warps: Einstein's outrageous legacy. 1994.
[60] M. Volonteri, M. Habouzit, and M. Colpi, Nature Reviews Physics **3**, 732 (2021)
[61] R. Tsuda, R. Suzuki, and S. Tomizawa, "Existence conditions of nonsingular dyonic black holes in nonlinear electrodynamics, " 8 2023.
[62] J. Barrientos, A. Cisterna, M. Hassaine, and K. Pallikaris, Phys. Lett. B **860**, 139214 (2025)
[63] B. Eslam Panah, A. Rincon, and N. Heidari, "Quasinormal modes and emission rate of ModMax (A)dS black holes, " 11 2024.
[64] J. F. Plebański and S. Hacyan, Journal of Mathematical Physics **20**, 1004 (1979)
[65] V. Bozza, Phys. Rev. D **66**, 103001 (2002)
[66] K. S. Virbhadra and G. F. R. Ellis, Phys. Rev. D **62**, 084003 (2000)
[67] K. S. Virbhadra, Phys. Rev. D **79**, 083004 (2009)
[68] K. Akiyama and *et al.*, AJ. **875**, 44 (2019)
[69] V. Bozza and L. Mancini, General Relativity and Gravitation **36**, 435 (2004)